Author Manuscript

Author Manuscript

Author Manuscript

Author Manuscript

HHS Public Access

Author manuscript

Abdom Imaging. Author manuscript; available in PMC 2017 June 27.

Published in final edited form as:

Abdom Imaging. 2015 October ; 40(8): 3161–3167. doi:10.1007/s00261-015-0530-9.

Motion Artifacts in Kidney Stone Imaging Using Single-Source and Dual-Source Dual-Energy CT Scanners. A Phantom Study

El-Sayed H. Ibrahim[1,2,*], **Joseph G. Cernigliaro**[1], **Robert A. Pooley**[1], **James C. Williams**[3], and **William E. Haley**[1]

[1]Mayo Clinic, 4500 San Pablo Rd, Jacksonville, FL 32224, USA

[2]University of Michigan, 1500 E. Medical Center Dr, Ann Arbor, MI 48109, USA

[3]Indiana University, 340 W 10th St, Indianapolis, IN 46202, USA

Abstract

Purpose—Dual-energy computed tomography (DECT) has shown the capability of differentiating uric-acid (UA) from non-UA stones with 90–100% accuracy. With the invention of dual-source (DS) scanners, both low- and high-energy images are acquired simultaneously. However, DECT can also be performed by sequential acquisition of both images on single-source (SS) scanners. The objective of this study is to investigate the effects of motion artifacts on stone classification using both SS- and DS-DECT.

Methods—114 kidney stones of different types and sizes were imaged on both DS-DECT and SS-DECT scanners with tube voltages of 80 and 140 kVp with and without induced motion. Postprocessing was conducted to create material-specific images from corresponding low- and high-energy images. The dual-energy ratio (DER) and stone material were determined and compared among different scans.

Results—For the motionless scans, all stones were correctly classified with SS-DECT, while two cystine stones were misclassified with DS-DECT. When motion was induced, 94% of the stones were misclassified with SS-DECT versus 11% with DS-DECT ($P < 0.0001$). Stone size was not a factor in stone misclassification under motion. Stone type was not a factor in stone misclassification under motion with SS-DECT, although with DS-DECT, cystine showed higher number of stone misclassification.

Conclusions—Motion artifacts could result in stone misclassification in DECT. This effect is more pronounced in SS-DECT versus DS-DECT, especially if stones of different types lie in close proximity to each other. Further, possible misinterpretation of the number of stones (i.e., missing one, or thinking that there are two) in DS-DECT could be a potentially significant problem.

[*]**Corresponding Author:** Dr. El-Sayed Ibrahim, *Assistant Professor*, Department of Radiology, University of Michigan, 1500 E. Medical Center Dr. (UH-B2-A209), Ann Arbor, MI 48109, USA, Telephone: +1-734-615-8003, Fax: +1-734-764-2412, elsayei@umich.edu.

Conflict of Interest: The authors declare that they have no conflict of interest.

Ethical approval: All procedures performed in studies involving human participants were in accordance with the ethical standards of the institutional and/or national research committee and with the 1964 Helsinki declaration and its later amendments or comparable ethical standards.

Informed consent: Informed consent was obtained from all individual participants included in the study.

Author Manuscript Author Manuscript Author Manuscript Author Manuscript

Keywords

Motion artifacts; Dual-energy computed tomography; Kidney stones; Nephrolithiasis

INTRODUCTION

Nephrolithiasis is a common chronic kidney disease, second only to hypertension [1]. Approximately 11% of men and 7% of women will have a kidney stone event in their lives and these numbers appear to be increasing [2]. Many of these patients are likely to be repeat stone formers with the likelihood of developing a second stone estimated to be 40% at 5 years and 75% at 20 years [3]. Nephrolithiasis is associated with high treatment costs, estimated at over $5 billion per year in the United States [4].

The majority of kidney stone patients present with flank pain requiring imaging for accurate diagnosis. Computed tomography (CT) has been established as the method of choice for kidney stone imaging with near 100% sensitivity [5]. Further, stone imaging with CT is fast and does not require the use of intravenous contrast material. Dual-energy computed tomography (DECT) is a more recently introduced imaging technique that acquires two CT data sets at two different energies, from which material-specific information can be obtained by exploring the energy dependence of attenuation coefficient for each material. DECT processing algorithm uses a three-material decomposition algorithm [6,7]. The dual-energy stone characterization technique has been shown to be capable of discriminating uric acid (UA) stones from other stone types with 90%–100% accuracy, depending on stone size and patient attenuation [8]. Use of DECT would thereby allow patients with UA stones to be treated medically and possibly avoid invasive interventional urinary procedures for stone removal or external shock wave lithotripsy.

DECT is performed on dual-source (DS) scanners by simultaneously acquiring low- and high-energy images, however, DECT can also be performed on single-source (SS) scanners by sequential acquisition of the low- and high-energy images [9]. During the CT scan procedure, the patient is instructed to remain still and hold his/her breath for about 30 seconds during the scan to avoid motion artifacts. Although motion artifacts generally result in distorted anatomy and blurring, in the case of stone imaging they may lead to misclassification of the stone type, as the dual-energy ratio (DER) would be altered if the low- and high-energy images are not exactly registered. Despite the importance of this type of artifact in stone imaging, very little attention has been paid to investigate this kind of artifact and characterize it in SS and DS scans, which is the purpose of this study.

METHODS

Phantom Preparation

One hundred and fourteen kidney stones passed or extracted from patients were obtained. The stone types (count) are as follows: apatite (15), brushite (14), calcium oxalate monohydrate (COM, 15), calcium oxalate dehydrate (COD, 15), cystine (16), struvite (15), UA (13), and mixed (8), as determined by micro CT analysis. The stones' size ranged from 2

Author Manuscript Author Manuscript Author Manuscript Author Manuscript

to 10 mm. An agarose phantom was created as follows (Figures 1 and 2). One hundred and fourteen 5-ml tubes were filled with an agarose-based material, created by dissolving 0.5% agarose in distilled water and doping the mixture with 0.085 milli-molar of MnCl2 to create a gel-like material mimicking the tissue properties of kidneys [10]. The tubes were heated for the agarose to completely dissolve in water, then left to cool down. Each stone was inserted inside a different tube when the gel-like material began to solidify.

Imaging Protocols

DECT images were acquired on Siemens dual-source (DS) FLASH scanner (equipped with tin filter for best separation of the spectra from the two energies) and single-source (SS) EDGE scanner (Siemens Healthcare, Forchheim, Germany) using renal stone imaging protocols. Four datasets were acquired on the DS scanner in two separate scans using tube voltages (kVp) of 80/140 (first/second datasets) and 100/140 (third/fourth datasets) in the first and second scans, respectively. The effective tube current-time products (mAs) were 18.5/8.5 (first/second datasets) and 9.5/10 (third/fourth datasets). Other scan parameters were constant for both scans: collimation = 19.2×0.6 mm and pitch= 0.7. The 80/140 kVp scan was repeated with exactly the same parameters as in the first 80/140 kVp scan, except that motion was induced during the scan. One of the authors, wearing a lead apron, stood at the rear of the scanner and used a plastic rod to softly shake the pillow on which the phantom resided in a consistent fashion in the table motion direction during scan.

Two datasets were acquired on the SS scanner in two separate scans using tube voltages (kVp)/effective tube current-time products (mAs) of 80/10.5 (first scan) and 140/10 (second scan). Other scan parameters were constant for both scans: collimation = 38.4 × 0.6 mm and pitch = 0.6. The two scans were repeated with same imaging parameters as in the first two, and with the same induced phantom motion as in the motion scan performed on the DS scanner.

The reconstruction parameters were the same for all datasets from the two scanners: reconstruction diameter = 20 cm, slice thickness = 0.75 mm, and slice interval = 0.5 mm using standard soft tissue reconstruction kernel. Syngo postprocessing software (Siemens Healthcare) was utilized to create material-specific images from corresponding low- and high-energy images (80/140 datasets or 100/140 datasets), whether the corresponding low- and high-energy images were acquired in the same scan (on the DS scanner) or in consecutive separate scans (on the SS scanner). The resulting color-coded images differentiate between UA and non-UA stones, which appear red and blue, respectively.

Imaging Analysis

The reconstructed CT images were transferred to a personal computer for analysis using commercially available software (RadiAnt; Medixant, Poland). For each stone in a given dataset, an ellipsoidal region-of-interest (ROI) was drawn inside the stone, where the average Hounsfield Unit (HU) was measured for the same ROI in both the low- and high-energy images. The dual-energy ratio (DER) was then measured for the stone by dividing the low-energy HU by the high-energy HU. The process was repeated for the motionless scans. The color-coded material-specific images produced by the scanners were inspected to

Author Manuscript Author Manuscript Author Manuscript Author Manuscript

determine the resulting UA/non-UA stone classification for all scans (with and without motion), where red, blue, and both blue and red represent UA, non-UA, and mixed stones, respectively. The stone type determined by the processing algorithm, described in [6–8], was compared to the known stone type.

RESULTS

Figures 3 and 4 show coronal images obtained without and with motion on the DS and SS scanners, respectively. Not all stones are shown on the images due to the different position of the stones inside each tube. Figure 3 shows the motion effect on DS-DECT, which resulted in repeated acquisition of the same row of stones (red rectangle in Figure 3(a)) that appeared twice (red rectangle in Figure 3(b)). Figure 4 shows the motion effect on SS-DECT, which resulted in misregistration of adjacent stones along the motion direction, as illustrated by the rectangles in the figure.

Table 1 summarizes the classification results and DER values for different stones and scans. For the motionless scans, all stones were correctly classified with SS-DECT, while two cystine stones were misclassified with DS-DECT at both energy levels. When motion was induced, 94% of the stones were misclassified with SS-DECT versus 11% with DS-DECT ($P < 0.0001$). In all scans, no UA stones showed as non-UA. Stone size was not a factor in stone misclassification under motion. Stone type was not a factor in stone misclassification under motion with SS-DECT, although with DS-DECT, cystine showed higher number of stone misclassification compared to other types.

As shown in Figure 5, the stone type affected DER with significant difference ($P < 0.0001$) between UA (DER ~ 1) and non-UA (DER > 1) stones. The stone size slightly ($P > 0.1$) affected DER, where the measured DER values were higher in the medium/large than in the small apatite stones, and was lower in the medium/large than in the small COD stones. The tube energy settings (on the same scanner) showed significant effect on DER for most stone types ($P < 0.005$), except for the UA and mixed stones, which was true for all stone sizes (small, medium, and larges). As shown in Figure 6, the DER values from the 80/140 scan always exceeded those from the 100/140 scan for DS-DECT. Similar results were obtained for the difference in DER between the DS- and SS-DECT (80/140 kVp settings), as shown in Figure 6. The difference was significant for most stone types ($P < 0.005$); but not for UA and mixed stones.

DISCUSSION

Motion artifacts may cause misinterpretation of kidney stones, especially when dual-energy algorithms are used to differentiate UA from non-UA stones. The current study shows that the imaging system (whether SS or DS) plays a significant role in the generated artifacts. The effect of imaging artifacts in DS-DECT is less than that in SS-DECT. The low- and high-energy images are simultaneously acquired in DS-DECT. Therefore, the motion effect is virtually the same on both images in DS-DECT, which prevents misregistration artifacts when both images are combined to generate the color-coded material-specific image. Nevertheless, motion may result such that certain anatomy is imaged twice or not imaged at

Author Manuscript Author Manuscript Author Manuscript Author Manuscript

all, depending on the nature and direction of motion during the scan. For kidney stone imaging, this artifact may lead to false negative or false positive results, as shown in Figure 3.

On the other hand, as the low- and high-energy images are consecutively, not simultaneously, acquired in SS-DECT, the motion effect would be different on both images, leading to misregistration artifacts when the images are combined together (Figure 4). This effect is accentuated when the stones are in close proximity to each other. Besides changing the shape and size of the imaged stones, misregistration artifacts would result in miscalculation of the stones' DER values and misinterpretation of their type. Further, stone disappearance or duplication is also possible on the combined image, as in the case of DS-DECT.

The significant difference in the percentage of misclassified stones between SS-DECT (94%) and DS-DECT (11%) reflects the difference in the nature by which the low- and high-energy images are acquired in both cases. Therefore, extra caution should be taken in SS-DECT to ensure that the patient remains still during the scan and the breath hold is maintained, as well as when interpreting the images. As shown in the results, all misclassifications in DS-DECT occurred as 'stone duplication' when one or more rows were scanned twice. Stones disappearance could have also occurred if motion results in skipping the scan of one or more rows. However, in the case of SS-DECT, image misregistration results in stone misclassification: UA or non-UA stones presented as mixed, or non-UA stones presented as UA; but in no case was a UA stone presented as non-UA. This finding agrees with the low HU range for UA stones, which ensures that DER does not exceed 1 if a UA stone in the low-energy image is misregistered with a non-UA stone in the high-energy image, and thus the stone is still classified as UA.

Besides the motion effect on stone identification, the kVp settings in DECT, as well as the system used appear to influence the DER values and stone classification, as shown for the cystine stones in the present study. Although the difference in DER based on the applied energies is expected, the inter-system (DS versus SS scanners) differences, despite the close setting of most scan parameters in both systems, are worth consideration. It should be noted that the UA DER values were very close in all scans, which did not affect the systems' capability for identifying UA stones. Although differences in the ROI used for calculating HU may contribute to some of the measurement differences, other system-specific factors, e.g. slight spectral overlap in DS-DECT, could be playing a role in these differences. Therefore, caution has to be taken when comparing images acquired on different systems, especially if parameter quantification is performed. Finally, to a lesser extent, stone size may affect DER, mainly due to partial volume effects. An additional difference between SS- and DS-DECT is the increased radiation dose in the former. However, we did not investigate this issue, as it has been previously investigated in another study by our group [11].

It should be noted that the measured DER values were significantly different between the two energy settings (80/140 or 100/140 kVp) on the same scanner, regardless of stone size, or type (except for UA and mixed stones). The trend was that DER values are always higher for the 80/140 kVp setting than for the 100/140 kVp setting. Nevertheless, the results here

Author Manuscript Author Manuscript Author Manuscript Author Manuscript

do not provide an evidence that one setting is better than the other. Actually, both settings are used for clinical care. For example, at our institution, we use 80/140 kVp and 100/140 kVp for imaging patients with cross-sectional diameters <35 cm and >35 cm, respectively, with satisfactory results in both cases.

Our study comes with agreement with a previous study by Grosjean et al [12], who investigated the influence of respiratory motion on renal stone characterization in vitro. Although both studies report significant motion effect on stone classification and recommend perfect breath-holding during in vivo scans, there are three differences between the two studies, as the study by Grosjean et al: 1) did not include small stones (all stones were larger than 7 mm in size); 2) did not study the effect of stone size on stone classification under motion; and 3) did not compare single-source to dual-source results. These issues have been addressed in our study, as explained in the previous section.

One limitation of the current study is that motion was induced subjectively and in one direction only. Although we expect the existence of similar artifacts in the case of patient motion in any direction during the scan, it is worth expanding the current study to include quantified motion induced in all three directions (e.g., using a motion phantom), which is one area of future work to expand on the findings from current study. Future research also includes comparing different stone classification algorithms from different scanner vendors to evaluate their susceptibility to motion artifacts. Finally, as any CT imaging protocol is associated with ionizing radiation, our future research involves investigating the capabilities of other imaging modalities for identifying kidney stones, e.g. magnetic resonance imaging (MRI) with the recently developed ultra-short echo-time (UTE) imaging sequences.

CONCLUSIONS

Motion artifacts could result in stone misclassification in DECT. This effect is more pronounced in SS-DECT versus DS-DECT as the low- and high-energy images are not acquired simultaneously, which may result in image misregistration, especially if stones of different types lie in close proximity to each other. Further, possible misinterpretation of the number of stones (i.e., missing one, or thinking that there are two) in DS-DECT could be a potentially significant problem.

References

1. Worcester EM, Coe FL. Nephrolithiasis. Prim Care. 2008; 35(2):369–391. vii. [PubMed: 18486720]
2. Scales CD Jr, Smith AC, Hanley JM, Saigal CS. Prevalence of kidney stones in the United States. Eur Urol. 2012; 62(1):160–165. [PubMed: 22498635]
3. Worcester EM, Coe FL. Clinical practice. Calcium kidney stones. N Engl J Med. 2010; 363(10): 954–963. [PubMed: 20818905]
4. Saigal CS, Joyce G, Timilsina AR. Direct and indirect costs of nephrolithiasis in an employed population: opportunity for disease management? Kidney Int. 2005; 68(4):1808–1814. [PubMed: 16164658]
5. Boulay I, Holtz P, Foley WD, White B, Begun FP. Ureteral calculi: diagnostic efficacy of helical CT and implications for treatment of patients. AJR Am J Roentgenol. 1999; 172(6):1485–1490. [PubMed: 10350277]

Author Manuscript Author Manuscript Author Manuscript Author Manuscript

6. Primak AN, Fletcher JG, Vrtiska TJ, Dzyubak OP, Lieske JC, Jackson ME, et al. Noninvasive differentiation of uric acid versus non-uric acid kidney stones using dual-energy CT. Academic radiology. 2007; 14(12):1441–1447. [PubMed: 18035274]

7. Matlaga BR, Kawamoto S, Fishman E. Dual source computed tomography: a novel technique to determine stone composition. Urology. 2008; 72(5):1164–1168. [PubMed: 18619656]

8. Boll DT, Patil NA, Paulson EK, Merkle EM, Simmons WN, Pierre SA, et al. Renal stone assessment with dual-energy multidetector CT and advanced postprocessing techniques: improved characterization of renal stone composition–pilot study. Radiology. 2009; 250(3):813–820. [PubMed: 19244048]

9. Leng S, Shiung M, Ai S, Qu M, Vrtiska TJ, Grant KL, et al. Feasibility of discriminating uric acid from non-uric acid renal stones using consecutive spatially registered low- and high-energy scans obtained on a conventional CT scanner. AJR Am J Roentgenol. 2015; 204(1):92–97. [PubMed: 25539242]

10. Ibrahim el SH, Rana FN, Johnson KR, White RD. Assessment of cardiac iron deposition in sickle cell disease using 3.0 Tesla cardiovascular magnetic resonance. Hemoglobin. 2012; 36(4):343–361. [PubMed: 22563880]

11. Jepperson MA, Cernigliaro JG, Ibrahim ES, Morin RL, Haley WE, Thiel DD. Vivo Comparison of Radiation Exposure of Dual-Energy CT Versus Low-Dose CT Versus Standard CT for Imaging Urinary Calculi. Journal of endourology/Endourological Society. 2014

12. Grosjean R, Sauer B, Guerra RM, Daudon M, Blum A, Felblinger J, et al. Characterization of human renal stones with MDCT: advantage of dual energy and limitations due to respiratory motion. AJR Am J Roentgenol. 2008; 190(3):720–728. [PubMed: 18287444]

Author Manuscript Author Manuscript Author Manuscript Author Manuscript

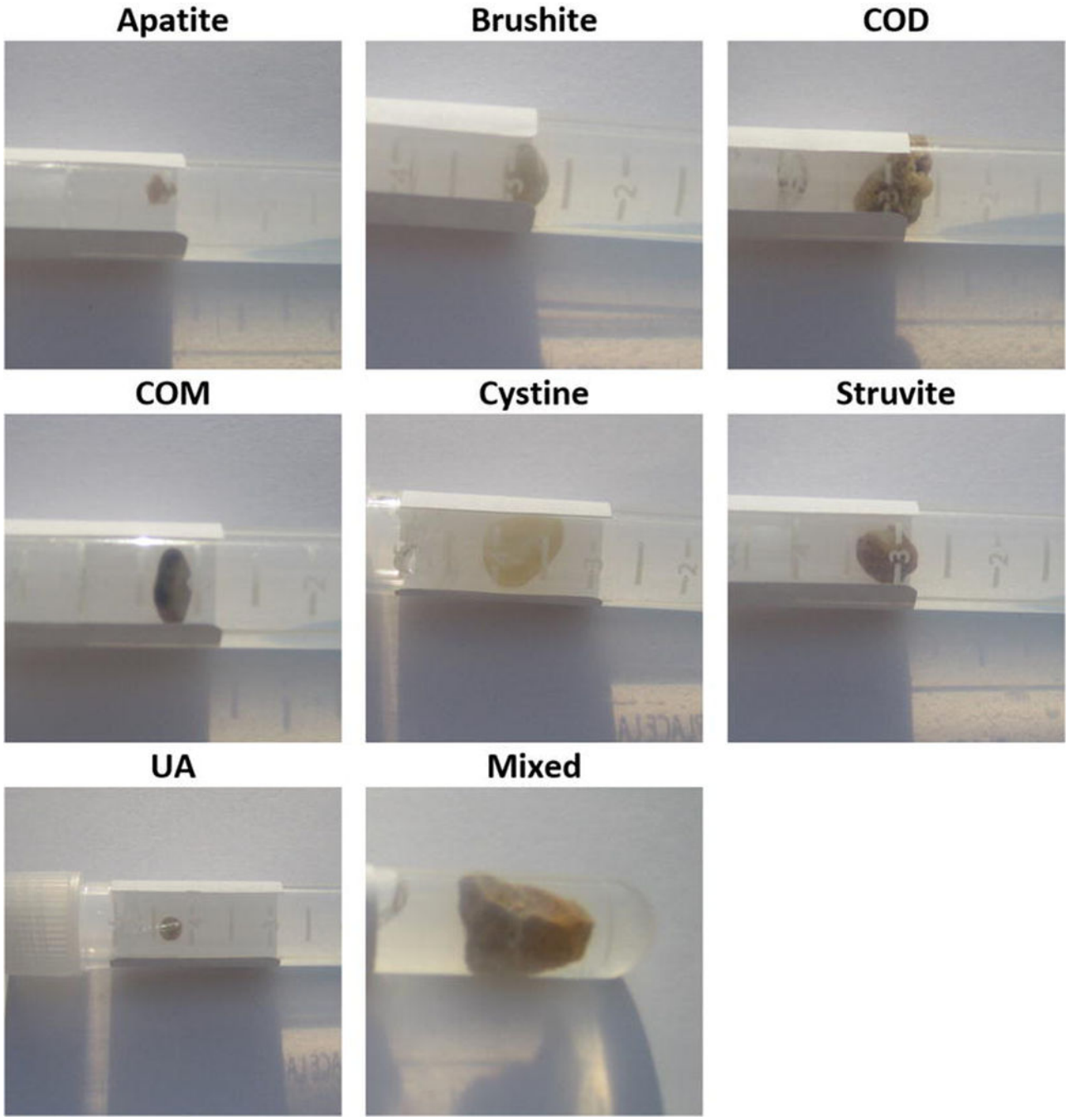

Figure 1.
Stones of different types and sizes. COD, calcium oxalate dehydrate; COM: calcium oxalate monohydrate; UA: uric acid.

Author Manuscript Author Manuscript Author Manuscript Author Manuscript

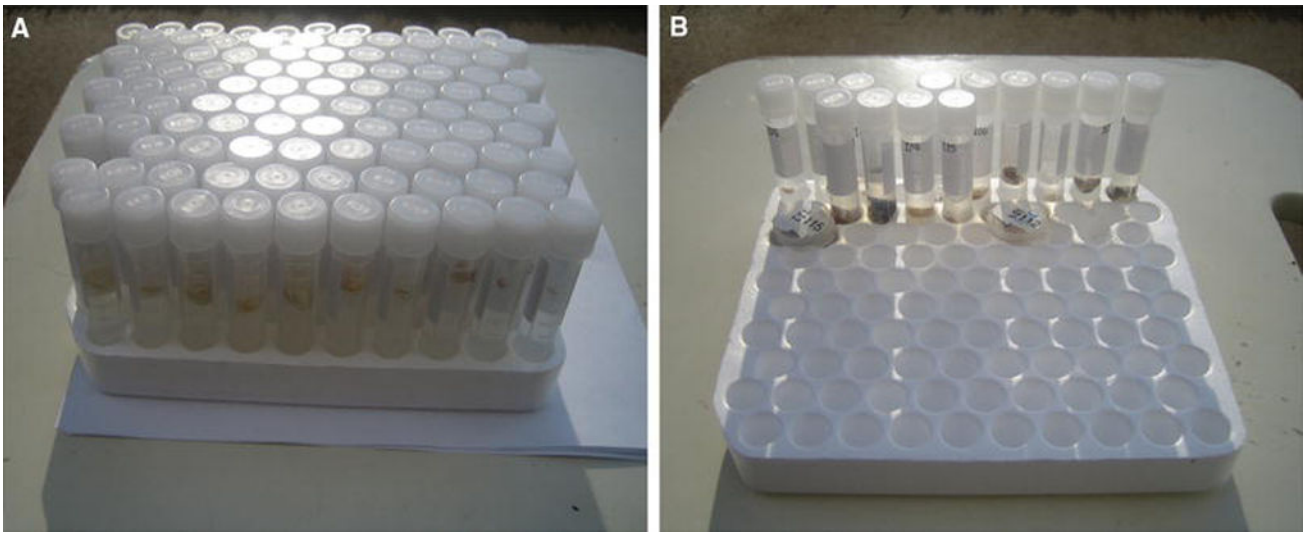

Figure 2.
Agarose phantom (bottom (a) and top (b) parts).

Author Manuscript Author Manuscript Author Manuscript Author Manuscript

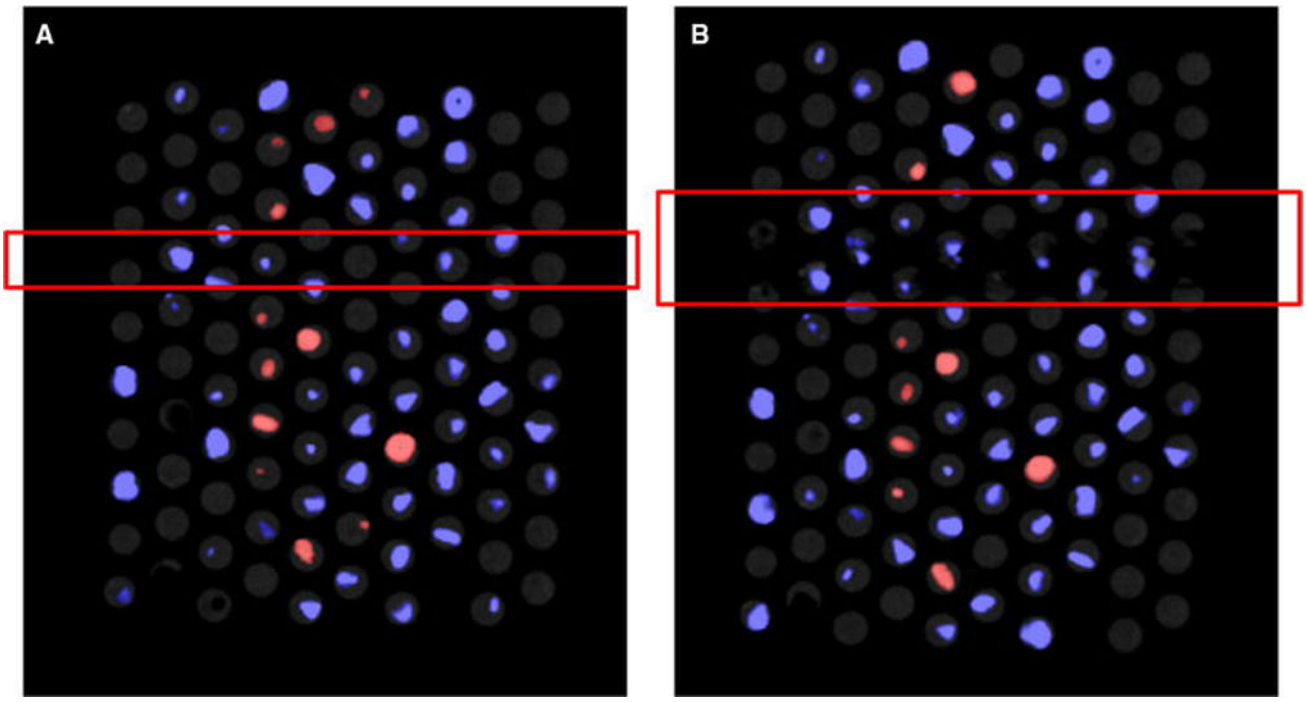

Figure 3.

Material-specific image of a coronal slice of the phantom showing different stones without (a) and with (b) motion, acquired with DS-DECT. Note that motion caused one row of stones to be scanned twice, which resulted in stone duplication (false positive). Red and blue colors represent uric acid and non-uric acid stones, respectively.

Author Manuscript Author Manuscript Author Manuscript Author Manuscript

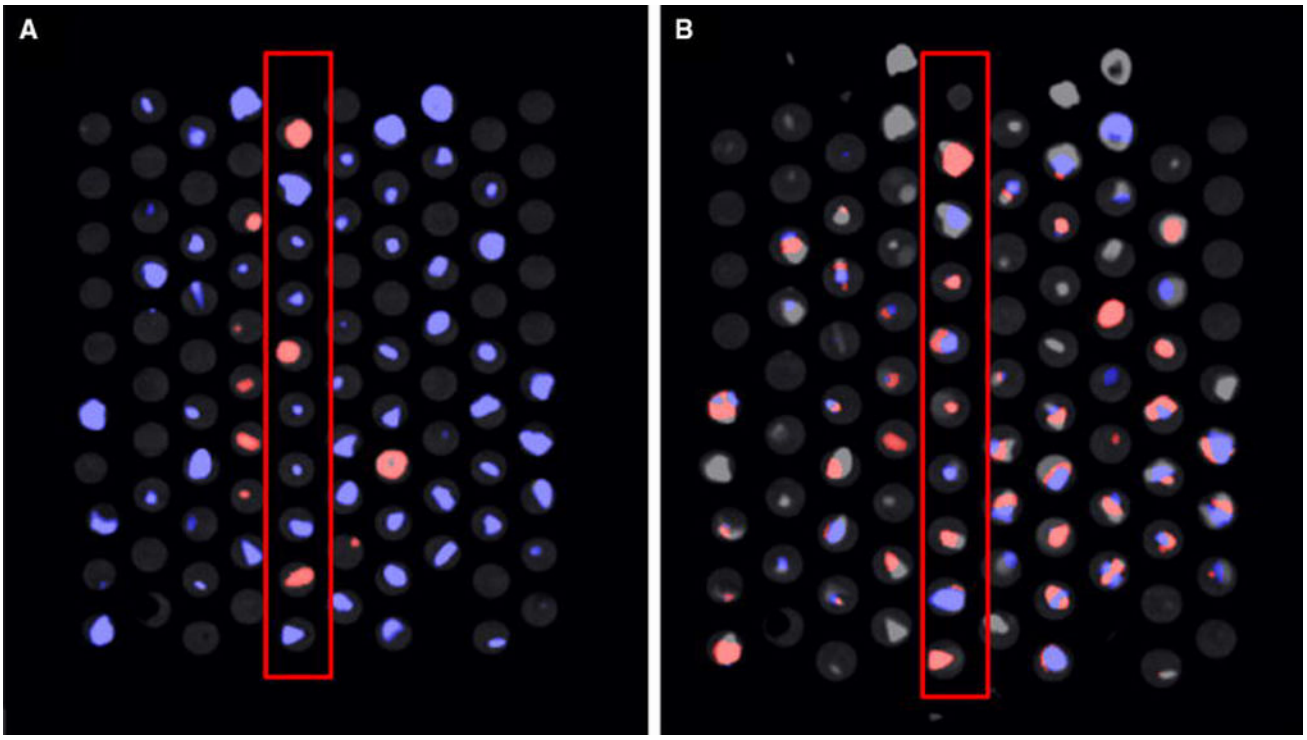

Figure 4.

Material-specific image of a coronal slice of the phantom showing different stones without (a) and with (b) motion, acquired with SS-SECT. Note that motion resulted in image misregistration, which lead to misclassification of most of the stones in the direction of motion (for example, see stones in the rectangle without and with motion). Red and blue colors represent uric acid and non-uric acid stones, respectively.

Author Manuscript Author Manuscript Author Manuscript Author Manuscript

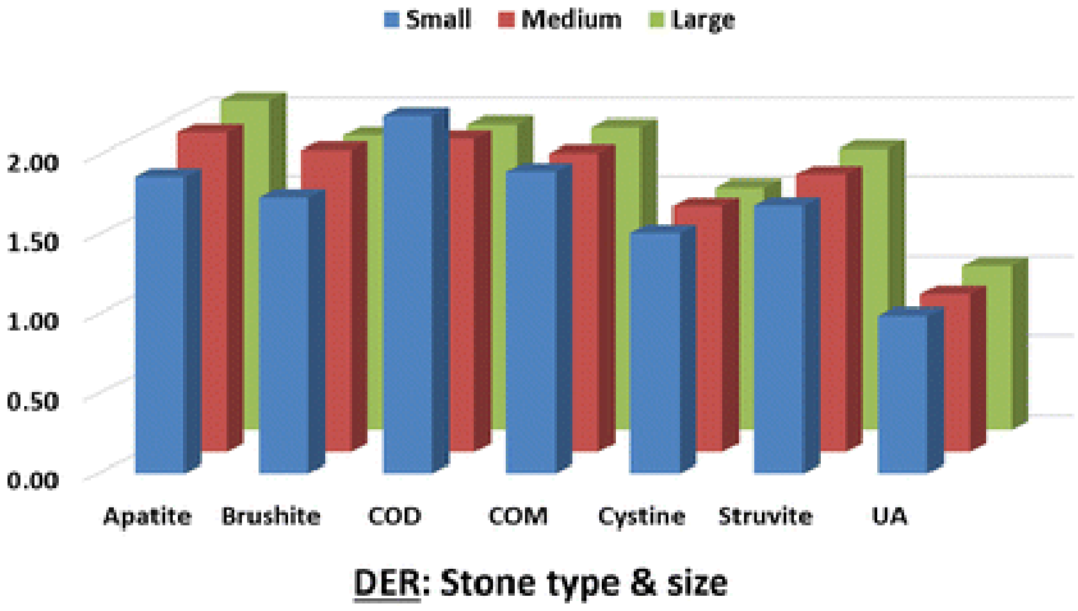

Figure 5.
The effect of stone size on dual-energy ratio (DER) of different stone types.

Author Manuscript Author Manuscript Author Manuscript Author Manuscript

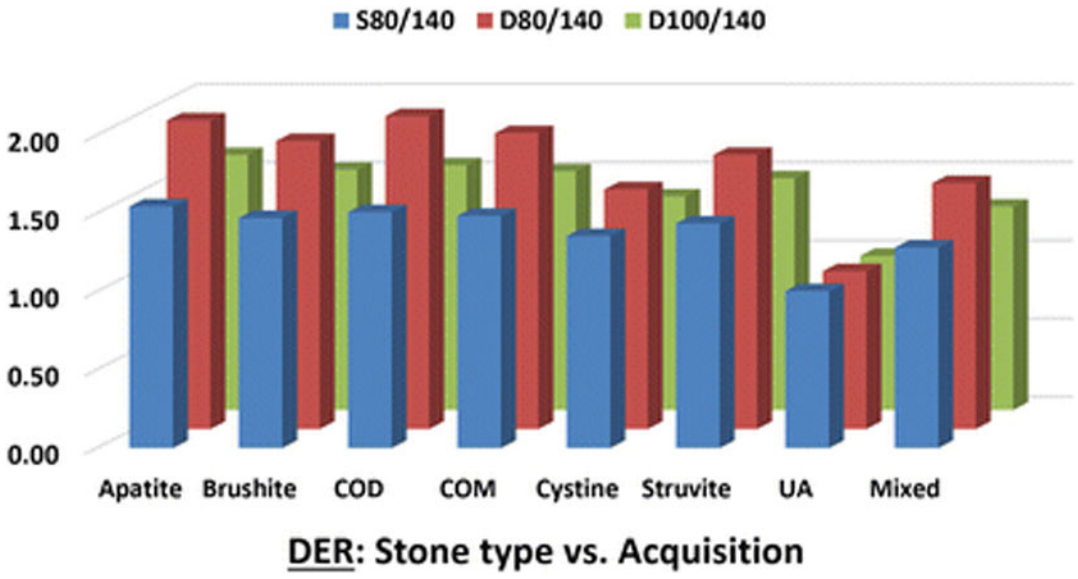

Figure 6.

The effects of energy settings (80/140 or 100/140 kVp) and system used (SS or DS) on DER of different stone types.

Author Manuscript Author Manuscript Author Manuscript Author Manuscript

Table 1

Stone types, size, dual-energy ratio (DER), and classification results.

Characteristics			# Misclassified Stones (UA/non-UA)					DER (Mean ± SD)		
			DS-DECT			SS-DECT				
Type	**Size (mm)**	**#**	**100 St**	**80 St**	**80 Mo**	**80 St**	**80 Mo**	**D100/140**	**D80/140**	**S80/140**
Apatite	2–3	6	0	0	1	0	6	1.65±0.13	1.86±0.14	1.58±0.15
	4–6	4	0	0	0	0	4	1.59±0.13	2.01±0.17	1.48±0.03
	7–10	5	0	0	0	0	5	1.64±0.04	2.07±0.12	1.55±0.11
Brushite	2–3	4	0	0	0	0	4	1.51±0.03	1.73±0.13	1.47±0.03
	4–6	6	0	0	0	0	6	1.53±0.03	1.9±0.02	1.48±0.01
	7–10	5	0	0	2	0	5	1.55±0.06	1.86±0.03	1.46±0.02
COD	2–3	4	0	0	0	0	4	1.59±0.09	2.25±0.27	1.55±0.11
	4–6	7	0	0	0	0	7	1.55±0.05	1.97±0.11	1.49±0.04
	7–10	4	0	0	1	0	4	1.57±0.04	1.92±0.04	1.5±0.03
COM	2–3	5	0	0	0	0	3	1.5±0.09	1.9±0.18	1.5±0.09
	4–6	6	0	0	1	0	6	1.54±0.03	1.88±0.06	1.48±0.03
	7–10	4	0	0	0	0	4	1.55±0.02	1.91±0.11	1.47±0.01
Cystine	2–3	2	0	0	0	0	2	1.34±0.01	1.51±0.08	1.37±0.04
	4–6	7	0	0	3	0	6	1.39±0.05	1.54±0.09	1.37±0.04
	7–10	7	2	2	2	0	7	1.34±0.07	1.53±0.12	1.33±0.07
Struvite	2–3	1	0	0	0	0	1	1.43	1.68	1.46
	4–6	7	0	0	1	0	7	1.45±0.04	1.74±0.17	1.4±0.07
	7–10	7	0	0	0	0	7	1.52±0.08	1.77±0.07	1.47±0.06
UA	2–3	5	0	0	0	0	5	1±0.03	0.99±0.06	0.98±0.06
	4–6	4	0	0	0	0	4	0.97±0.02	0.99±0.04	1±0.06
	7–10	6	0	0	1	0	6	0.98±0.04	1.03±0.13	1.02±0.15
Mixed	7–10	8	0	0	1	0	5	1.3±0.23	1.57±0.42	1.28±0.21

Abdom Imaging. Author manuscript; available in PMC 2017 June 27.

Author Manuscript Author Manuscript Author Manuscript Author Manuscript

Characteristics			# Misclassified Stones (UA/non-UA)						DER (Mean ± SD)		
			DS-DECT			SS-DECT					
Type	Size (mm)	#	100 St	80 St	80 Mo	80 St	80 Mo	D100/140	D80/140	S80/140
Total		114	2	2	13	0	107			

Abbreviations: St, stationary; Mo, motion; D, dual-source; S, single-source.